This is the accepted manuscript of the following publication: K. A. Villarreal Chaires, E. Barocio, D. Del Puerto Flores, F. R. S. Sevilla and P. Korba, "A Geographic Information System Application to Estimate the Weather-Dependent Power System Losses," 2021 IEEE International Autumn Meeting on Power, Electronics and Computing (ROPEC), Ixtapa, Mexico, 2021, pp. 1-7, doi: 10.1109/ROPEC53248.2021.9668064.

A Geographic Information System Application to Estimate the Weather-Dependent Power System Losses

Karen Villarreal, Emilio Barocio, Dunstano del Puerto Flores
Graduated program in electrical engineering
Universidad de Guadalajara
Guadalajara, Jalisco, Mexico
emilio.barocio@academicos.udg.mx

Felix Rafael Segundo Sevilla, Petr Korba
Electric Power Systems and Smart Grid Lab
Zurich University of Applied Sciences ZHAW
Winterthur, Switzerland

***Abstract*— The accuracy of weather-dependent power flow analysis for large interconnected systems can be significantly improved by including more electrical devices exposed to weather variables such as ambient temperature, wind speed and solar irradiance. The innovative part of the proposed approach is the combination of factors such as a voltage regulating transformer model, freely available weather data to feed the weather-dependent power flow algorithm, and a geographic visualization tool to display the results. To demonstrate the effectiveness of the proposed approach, the IEEE 118-bus system is used to analyze and compare the results of the weather-dependent power flow model versus a conventional power flow. In this case, it is used in the stationary analysis, the power flow temperature algorithms are performed in spatial visualization schemes. The results show that weather conditions directly affect the power system performance.**

***Index Terms*-- weather-depend power flow solution, open weather collection system, weather effects, visualization tools.**

I. Introduction

In recent years, large interconnected power systems (LIPS) have experienced equipment damage and service disruptions due to extreme weather conditions. This vulnerability of LIPS to extreme climate changes is also a potential danger to the stability of the transmission grid [1]. The United Nations (UN) already foresees problems in the electricity sector caused by abrupt changes in temperature levels worldwide, i.e. more than 0.1ºC of climate anomaly per year [2]. During the summer 2020, in the state of California in the US, temperatures reached 40°C for several days, causing power outages for more than 410,000 customers [3]. For these reasons, power system utilities urge for advanced tools that integrate climate change and guarantee a secure planning, design, analysis and control.

In the literature, there is a very limited number of studies that demonstrates that an increase on temperatures actually reduce the transmission capacity of overhead lines [4][5]. Resistance and temperature in the conductors and correlated meteorological variables such as ambient temperature, wind speed and solar irradiation [6] are directly related to transmission line losses, even under normal operating conditions [7]. In [8] the authors show that changes in the resistant of the transmission lines, caused by temperature variations, produce errors of up to 10% under high-loading conditions. The relevance of incorporating accurate parameters such as line resistance and meteorological variables in the analysis of energy systems has been acknowledge in several studies of the literature. It is important to mention that when it comes to the inclusion of climate in the Dynamic Thermal Rating (DTLR) studies, these are only for the study of a limited number of transmission lines [9][10

In [7] and [11], it is proposed a power flow formulation considering meteorological conditions. In these works, an estimation of the temperatures and resistances of the lines are combined with conventional power flow equations. In [8] the use of line resistance and temperature for state estimation is reported, resulting on more accurate estimation of the states variables of the system. In [4] and [12], it was observed that weather conditions have a direct impact on the electrical load and that variability of meteorological conditions introduce additional constraints, when predicting behavior of transmission lines. In [13] an optimal power flow algorithm based on meteorological conditions with wind farm integration was presented to consider the interdependence between temperature resistance and dynamic capacity of overhead lines. Recently in [14], the effects of meteorological conditions on transient stability problems considering several conductors were presented. The aforementioned studies establish the advantages of using weather-dependent transmission line models in contrast with conventional tools.

Reduction of electric power losses during its transmission on power lines is one of the priorities of the electric power industry development. According to the Strategy for the Development of the Power Grid of the Russian Federation, the improvement of operational efficiency is associated with the implementation of measures aimed at reducing losses of electric power during its transmission on power lines. Electric power losses during transmission and distribution power lines amount to about 14-17% of the productive supply [15], These data give us an idea of the importance of active power losses.

Authors with CVU numbers 957921 and 30951 express their gratitude to the Mexican National Council for Science and Technology (CONACYT) for the financial support through the graduated program scholarship and national program “Sistema Nacional de Investigadores”.

Moreover, incorporation of weather conditions in the mathematical formulation could lead to a potential reduction of the total generation costs, maximization of overhead lines capacity and quantification of total power losses. Finally, although available software tools such as PowerWorld [16], dynamic security evaluation [17] using TSAT™, or transient stability [18] using Cyme are already introducing visualization instruments, these programs do not consider weather conditions.

This paper presents an extension of the power flow formulation of the works in [7] and [11], considering the meteorological effects on regulating transformers within the power flow formulation as a first approximation. Additionally, a system for collecting meteorological data from a freely available database that feeds the power flow formulation is developed and a cost-effective way of data updating is proposed.

As mentioned above, there is a tendency to implement visualization tools to facilitate the interpretation of results for power grid operators and planners, so this work proposes a complementary visualization tool, which allows obtaining results such as energy losses and temperatures in transmission lines and other elements such as transformers, considering the updated climatic effects, visualized geographically.

It is important that this work focus on the modeling of the climatic dependence of the electrical resistance of the conductor incorporating the dependence, because it is only of interest for the moment of the analysis of the electrical losses of active power, due to the great importance that these have for the electrical industries.

II. TEMPERATURE-DEPENDENT (TD) MODEL OF OVERHEAD TRANSMISSION LINES

In general, the electrical network is composed of different assets such as generators, transformers, overhead lines and loads, as illustrated on Fig. 1. The electric components can be represented using impedance models ($Z = R + jX$) for steady-state simulations, where Z is the impedance, R is the electrical resistance and X is the reactance of the conductor.

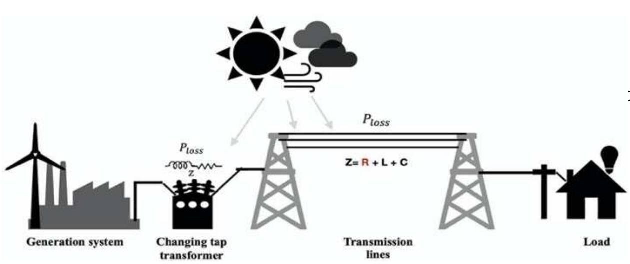

Figure 1. Representation of different assets in an electrical network

The parameters of the impedance model have direct influence on the transmission capacity of the power flow. In particular, conductor resistance and weather changes contribute to have significant transmission losses. The resistance of a metallic conductor is proportional to its temperature [19].

$$R(T_c) = R_{ref} \frac{T_c + T_F}{T_{amb} + T_F} \tag{1}$$

This thermal model is taken from [7], where $R(T_c)$ is the conductor resistance, R_{ref} is the resistance at refence temperature. T_F is the reference temperature, T_c conductor temperature and T_{amb} is the ambient temperature Eq. (1) calculates the conductor resistance for a given reference point (R_{ref}, T_F and T_{amb}) and the present device temperature (T_c). However, to incorporate the thermal effects on the resistance model, it is assumed that the increase of the conductor temperature is linearly proportional to the heat flowing out in the conductor i.e. losses in the conductor. As in [19], R_θ is the steady-state temperature rise ratio:

$$R_\theta = \frac{T_{inc}}{P_{loss}} \tag{2}$$

where T_{inc} is the rising conductor temperature above ambient level and P_{loss} is the total loss of the conductor in the transmission line.

Now, assuming that the temperature of the conductor T_c is defined as the sum of the ambient temperature and the rise of the conductor temperature, yields:

$$T_c = T_{amb} + T_{inc} \tag{3}$$

Solving (2) for T_{inc} and substituting into (3), yields the nonlinear algebraic equation defined as follows:

$$T_c - (T_{amb} + R_\theta P_{loss}) = 0 \tag{4}$$

Eq. (4) can be solved using any iterative numerical method such Newton-Rapshon. The total loss in the device is calculated as:

$$P_{loss} = I^2 R(T_c) \tag{5}$$

where I is the current flowing through the conductor and $R(T_c)$ is the thermal resistant model depending on the conductor temperature variation during one day. Using the concepts defined on Eq. (1) to (5), the total power active losses for an overhead line conductor is:

$$\begin{aligned} P_{loss,ij} = P_{ij} + P_{ji} &= Re\{V_i I_{ij}^* + V_j I_{ij}^*\} \\ &= g_{ij}(V_i^2 + V_j^2 - 2g_{ij}V_iV_j\cos(\delta_i - \delta_j) \end{aligned} \tag{6}$$

where, g_{ij} is the conductance and V_j and δ_i are the magnitude and the angle of the bus voltage, respectively, and i and j are the nodes of the line to be analyzed. The conductance and susceptance of a branch ij are functions of the branch resistance and reactance as shown in (7). It is worth noticing that the temperature effects on $P_{loss,ij}$ are contained on the conductance parameter defined as:

$$g_{ij} = \frac{R_{ij}(T_c)}{R^2{}_{ij}(T_c) + X^2{}_{ij}}. \tag{7}$$

From Eq. (7), the influence of impedance parameters can be observed; $R_{ij}(T_c)$ associated to the power systems losses and X_{ij} associated to inductance and capacitance to help inducing the regulated voltage on the system.

Finally, an energy balance that can be represented into the TD power flow solution is obtained by substituting (6) into (4) results in:

$$H_{ij}{}^{calc} = T_{c,ij} - (T_{amb,ij} + R_{ij} * (g_{ij}(T_C)(V_i{}^2 + V_j{}^2 - 2g_{ij}(T_C)V_iV_j\, cos(\delta_i - \delta_j)\,) \quad (8)$$

The values obtained from the weather collection system for the ambient temperature T_{amb} given in Eq. (1), affect directly T_c and subsequently the conductor resistance $R(T_c)$.

III. Weather-dependent (WD) model of overhead transmission lines

The relationship between the line conductor and variations on the weather conditions can be accurately modelled using the non-linear thermal equilibrium equation introduced on [19], regularly used to perform dynamic thermal line classification (DTLR), therefore the heat balance is defined as

$$q_c + q_r = q_s + q_j \quad (9)$$

This thermal model is taken from [11], where q_c is the energy loss by convection, q_r is the energy loss by radiation, q_s is the energy gain by solar irradiation, and q_j is the energy loss by Joule effect, that is,

$$q_j = P_{loss} \quad (10)$$

The loss of convective energy in this work has an important role due to the geographical area, the season of the year and the recent climate change, the winds that occur in some parts are predominant. Therefore, it is important to mention the influence that the wind speed, V_w, has on q_c as follows

$$q_c = K_a\left[1.01 + 1.35 * \frac{D_0\rho_f V_w{}^{0.52}}{\mu_f}\right]k_f(T_c - T_{amb}) \quad (11)$$

where K_a is the wind direction factor, D_0 is the diameter of the conductor, ρ_f is the density of the air, μ_f is the absolute viscosity of the air, k_f is the thermal conductivity of the air and T_{amb} is the ambient temperature. Some variables depend on the case of design values and therefore are considered constant as D_0 and K_a, others such as ρ_f, μ_f and k_f are obtained by preset equations which depend on constant design values, and geographical location of the conductor and T_{amb}, and generally are relatively small in relation to T_{amb} and V_w,. In relation to the above, it is observed from (11) that there are only two weighting variables, T_{amb} and V_w,, which reach values from -8 to 40ºC and 0 to 50 km/h, respectively.

The following expression relates the electrical losses of the transmission line with the heat balance equation:

$$q_c + q_r - q_s - \big(g_{ij}(T_C)(V_i{}^2 + V_j{}^2) - 2g_{ij}(T_C)V_iV_j\cos(\delta_i - \delta_j)\,\big) = 0 \quad (12)$$

The electrical resistance of an overhead conductor in the admittance matrix, is adjusted linearly to the temperature of the conductor's surface and can be found by linear interpolation using (13) as reported in [19]:

$$R(T_c) = \left[\frac{R(T_{high}) - R(T_{low})}{T_{high} - T_{low}}\right](T_c - T_{low}) + R(T_{low}) \quad (13)$$

where the high and low temperatures, T_{high} and T_{low}, are used. The literature presents different equations for the calculation of convection, irradiation and solar energy. In this work those developed in IEEE Std 738TM-2012 [19] are used.

IV. Generalized Climate-dependent power flow formulation

In this section, an extension to the results reported in [7] and [11] are presented. In the former documents, the results of the formulation of polar power flow including temperature and weather models were developed and compared. Following the definitions given in [7] and [11]; in the subsequent par this document, the temperurate-dependent power flow (TD-PF) and weather-dependent power flow (WD-PF) notation are used to identify the power flow model used in the simulations. Here, motivated by the need of nodal voltage regulations, a formulation of power flows with weather-dependent tap changing transformers are considered.

A. Power transformer model

Uncontrolled voltage drops are becoming more and more frequent in the electrical system as a consequence of the continuous growth of energy consumption, the sudden disconnection of transmission and generation elements, and sudden load variations by tap-changing transformers [20]. However, devices as well as many other elements that make up the electrical network are affected by the weather such as transmission lines. Therefore, this section incorporates the regulating transformer formulation with the model explained in Section II, in which only the analysis of the transformer windings is assumed as a first approximation to integrate the climate impact of these elements within power flows.

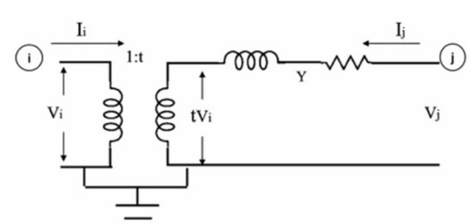

Figure 2. Electric diagram of a tap changer transformer.

The starting point is the analysis of figure 2. Based on currents and voltages ratios of the transformer model described in (12), the equivalent circuit is defined as follows:

$$\begin{bmatrix} I_i \\ I_j \end{bmatrix} = \begin{bmatrix} Y_{ii} & Y_{ij} \\ Y_{ji} & Y_{jj} \end{bmatrix} \begin{bmatrix} V_i \\ V_j \end{bmatrix} = \begin{bmatrix} t^2 * Y(T_c)_T & -t^* Y(T_c)_T \\ -Yt & Y \end{bmatrix} \begin{bmatrix} V_i \\ V_j \end{bmatrix} \quad (14)$$

where t is the value of the tap and $Y(T_c)_T$ is the admittance of the regulating transformer.

In this document, the tap *t* is considered an independent parameter with a specified value. Each regulating transformer is modeled as a load node. Furthermore, an additional row and column are integrated to the original admittance matrix, representing the incorporation of an additional node *m,* where *m* is the number of regulating transformers. The result is a new admittance matrix of larger dimension:

$$Y = \begin{bmatrix} Y_{11} & Y_{1i} & Y_{1j} & 0 \\ Y_{i1} & t^2 * Y(T_c)_T + Y_{ii} & Y_{ij} & -t * Y(T_c)_{T(i,m)} \\ Y_{j1} & Y_{ji} & Y_{jj} & 0 \\ 0 & -t * Y(T_c)_T & 0 & Y(T_c)_{T(m,m)} \end{bmatrix} \quad (15)$$

To simulate the effects of the temperature into the regulating transformer windings, the TD model described in Section III is used.

It is important to mention that it is necessary to introduce in the future more detailed models of the transformer, since this paper was introduced as a first approach to the study of more elements considering climate dependence.

B. *Climate-dependent power flow equations*

In a conventional power flow calculation, two state variables are estimated for each bus of the system: magnitude and voltage angle. From these state variables the active and reactive power at each bus is calculated [22]. When the environmental conditions are integrated in the flow formulation, an additional state variable is incorporated, which is associated to the temperature conductor temperature, in this case the temperature of the transmission lines, T_c, and calculated using the TD and WD models introduced on sections III and IV, respectively. The extended state variable vector is defined as:

$$\boldsymbol{x} = \begin{bmatrix} \boldsymbol{\delta}_{n-1} \\ \boldsymbol{V}_{n_D} \\ \boldsymbol{T}_{c_{n_l}} \end{bmatrix} \quad (16)$$

$$n_D = n_{load} + n_T$$
$$n = n_D + n_G$$

where n_D is the number of loading nodes including the node of the transformers, n_G is the number of generation nodes, n_l is the number of lines. The power error vector is reformulated as follows:

$$\boldsymbol{f}(\boldsymbol{x}) = \begin{bmatrix} \Delta \boldsymbol{P}_{i\,n-1} \\ \Delta \boldsymbol{Q}_{i\,n_D} \\ \Delta \boldsymbol{H}_{ij\,n_l} \end{bmatrix} = \begin{bmatrix} \boldsymbol{P}_i^{esp} - \boldsymbol{P}_i^{calc} \\ \boldsymbol{Q}_i^{esp} - \boldsymbol{Q}_i^{calc} \\ \boldsymbol{0} - \boldsymbol{H}_{ij}^{calc} \end{bmatrix} \quad (17)$$

where $\boldsymbol{H}$ for the regulating transformer is calculated from equation (8) and for the climate-dependent transmission line from (12), $\boldsymbol{P}$ is the active power and $\boldsymbol{Q}$ is the reactive power.

For the construction of the Jacobian matrix, the addition of $\boldsymbol{T}$ to the state vector is considered, which causes an increase in the size of the Jacobian matrix, that is,

$$\boldsymbol{J}(\boldsymbol{\delta}, \boldsymbol{V}, \boldsymbol{T}) = \begin{bmatrix} \frac{\partial \boldsymbol{P}}{\partial \delta_{n-1xn-1}} & \frac{\partial \boldsymbol{P}}{\partial V_{n-1xn_D}} & \frac{\partial \boldsymbol{P}}{\partial T_{c_{n-1xn_l}}} \\ \frac{\partial \boldsymbol{Q}}{\partial \delta_{n_Dxn-1}} & \frac{\partial \boldsymbol{Q}}{\partial V_{n_Dxn_D}} & \frac{\partial \boldsymbol{Q}}{\partial T_{c_{n_Dxn_l}}} \\ \frac{\partial \boldsymbol{H}}{\partial \delta_{n_lxn-1}} & \frac{\partial \boldsymbol{H}}{\partial V_{n_lxn_D}} & \frac{\partial \boldsymbol{H}}{\partial T_{c_{n_lxn_l}}} \end{bmatrix} \quad (18)$$

Once the equations of the power, TD and WD models of the regulating transformer and transmission lines are defined, the updated equation is used to obtain the magnitude and angle of the voltages, and the temperatures of the lines on the system,

$$\begin{bmatrix} \boldsymbol{\delta} \\ \boldsymbol{V} \\ \boldsymbol{T}_C \end{bmatrix}^{k+1} = \begin{bmatrix} \boldsymbol{\delta} \\ \boldsymbol{V} \\ \boldsymbol{T}_C \end{bmatrix}^{k} + \boldsymbol{J}(\boldsymbol{\delta}, \boldsymbol{V}, \boldsymbol{T}_C)^{-1} * \begin{bmatrix} \Delta \boldsymbol{P} \\ \Delta \boldsymbol{Q} \\ \Delta \boldsymbol{H} \end{bmatrix} \quad (19)$$

V. INTEGRATION OF OPEN ACCESS WEATHER MONITORING SYSTEMS

Access to free and virtual information of meteorological monitoring systems for collection of data make possible to have weather-dependent power flows. Open access information does not require additional equipment installed in the electrical network, and make possible to have fresh and updated data continuously.

Although every meteorological variable is relevant for a successful calculation, based on a heat balance analysis from (9), variables can be classified according to its nature and importance. The classification used here is depicted on Fig. 3 and different type of variables are observed: constants variables (in yellow) that are obtained using the location of the equipment or by design values, calculable variables (in blue), non-measurable variables (in purple) and measurable variables (in red). The latest ones are obtained from meteorological open access databases. Fig. 3, also shows the connectivity of the variables and identifies the values that need to be accessed through the database of geographical and physical characteristics of the lines. The information can be considered constant unless there is a geographical change in the network. Non-measurable variables, and measurable variables are obtained from public databases.

Measurable variables are wind speed (V_w), wind direction (λ) and ambient temperature T_{amb} and can be accessed as follows:

- Wind speed, wind direction and ambient temperature can be obtained from the MEREORED [23] and OPENWHEATHER [24] databases, which are updated every hour. These are freely accessible databases, which works with the European Centre for Medium Term Weather Forecasts (ECMWF) prediction model based on the collection of atmospheric data with satellite remote sensing.
- Electrical variables such as node voltage angles and magnitudes can be accessed from a SCADA system with resolution of 1 second [25] in conjunction with a state estimation algorithm.

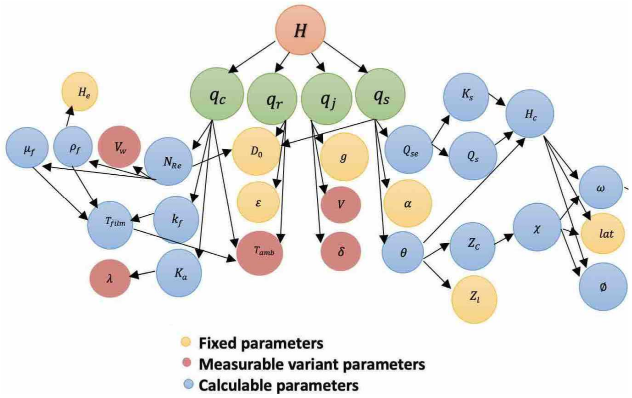

Figure 3. Variable connectivity diagram for each day at a particular time

The proposed algorithm of power flows considering WD is updated every hour, assuming as constant values the solar radiation until a new update is available. An average of the voltage magnitude and angle of each bus is computed every hour. It should be noted that in order to have access to databases it is necessary to have latitude and longitude of the transmission lines.

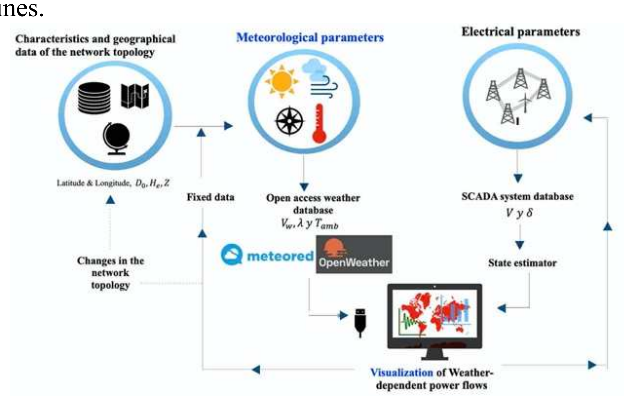

Figure 4. Diagram for implementation of climate-depend power flow into the control center.

The diagram depicted on Fig. 4 is used to illustrate how the data that feeds the algorithm is obtained. The updated time scales for the algorithm are considered applicable for different studies of the network, for load distribution forecasts and economic dispatch, especially when it is necessary to integrate wind generation unit.

VI. Numerical Results

A. System test data and geo-climatic visualization

To show the effectiveness of the proposed formulation in a large-scale power system, the IEEE 118-buses system is used, and it consists of 19 generators, 91 loads and 9 transformers. The model approximates the Midwest system in the US.

In addition, for the purpose of validation and simplification of the interpretation of the algorithm results, and to provide a complementary visualization tool for network operators, the results of active and reactive power losses, as well as line and transformer temperatures, are shown below, where these results can be visualized considering geoclimatic information.

The geo-climatic visualization consists of a combination of the POWERMAP software used for the visualization and BING for the virtual geographic base [26] to display the results. An overlap of the IEEE system with the actual geographical location in the US is presented where the following data was used for the system:

The initial conditions of power flows are at [27] and the geospatial transmission lines and nodes of the system were distributed according unifiliar diagram of this system, all transmission lines are 200 km longitude, conductors are 795 cmil 26/7 ACSR, constant load and generation data, transformer reactance 0.02 p.u with t=1.05 s, 100ºC as thermal limit of the lines, $T_F = 241$ ºC of copper for the transformer windings and $T_F = 228.1$ ºC for the power supply in the transmission lines, emissivity and absorptivity =0.8 p.u, elevation above sea level $H_e = 0$ m. Table I summarize the measurable parameters for a specific day and time during the 2019 summer in the US (14.06.2019 at 4:00 p.m.). Temperature data was taken uniformly throughout each state [17]. Similarly, wind speed was used uniformly across each state for the same date, Table I.

Table I. CLIMATE DATA FOR THE MIDWESTERN STATES (US).

Zone	State	Latitude	Wind speed km/h	Temperature ºC
1	Minnesota	44.881	26	29.6
2	Iowa	41.533	20	20
3	Missouri	43.913	25	28
4	Illinois	41.785	20	27
5	Indiana	39.718	26	23
6	Ohio	39.998	28	23
7	Wisconsin	42.948	38	26
8	Michigan	42.408	16	22

B. Simulation results

Fig. 5 summarizes the comparison of the active power losses for the conventional formulation, i.e. the one that considers the value of the electrical resistance of the conductors based on an equation with fixed temperature, in the professional software DIgSILENT PowerFactory, the TD-PF, which as described in Section II is based on a temperature model and finally the WD-PF, which considers different environmental values such as ambient temperatures, wind speed, solar radiation, among others.

In addition, fig. 5 shows the active power losses obtained with the three different formulations in the form of a bar graph. It can be seen that the WD-PF formulation in most of its lines shows higher values compared to the TD-PF and DIgSILENT results, due to the ambient temperature and wind speed that occur in some areas of the Midwest of the United States.

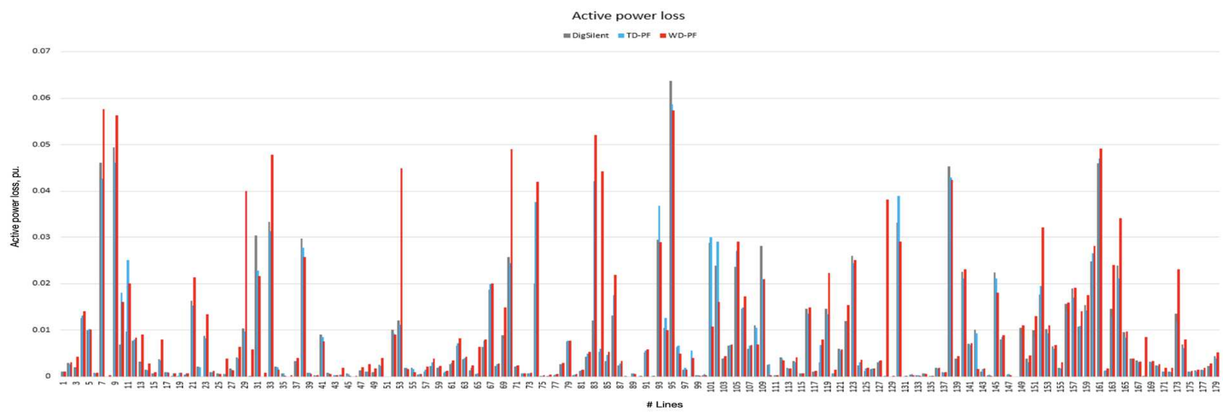

Fig. 5.- Active power losses in transmission lines, 118-nodes

For example, in the state of Minnesota the highest ambient temperature of approximately 30°C can be found, which is reflected on the corresponding active power losses. The result is in agreement with the magnitude of the red bars (representing WD-PF). On the other hand, the active power losses from WD-PF in Wisconsin are smaller than the blue bars (TD-PF) as result of the strong wind speeds. Note that in the results depicted on Fig. 5, long transmission lines or those located close to large loads or generators, have significantly higher temperatures and more active power losses, this is due to the fact that these are long transmission lines, approximately 400 km long, with high demands and therefore produce higher losses.

However, it can be seen in the comparison of the three formulations where WD-TD are the red bars, TD-PF are the blue bars and finally the gray bars correspond to DigSilent. The increase of active power losses in the case of WD-TD and TD-PF are remarkable and this is due to the variation of ambient temperatures in some areas and to the different wind speeds. The usefulness of the latter graphs is still limited, when it comes to quickly and completely detect not only the results but also the different variables that influence these results, for example the geographical area where the elements are located and the main climatic variables that affect them.

As a complementary tool, a way of visualizing the results is presented below, the results are shown in a geo-climatic visualization, Figure 6, shows the active power losses in the test case of 118 buses comparing the system with regular transformers (yellow bars) and without them (blue bars). Where it can be seen only in some nodes the improvement in the accuracy of results considering this formulation. in which the transmission lines and transformers are geographically located and the results are projected. This is intended to provide a complementary form of visualization for power system operators and planners.

This form of visualization allows to give a first approximation of the electrical losses or of some other important variable that involves the climate according to the day or certain season of the year.

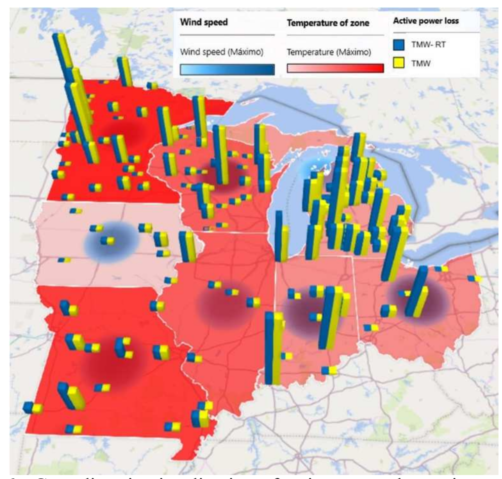

Fig. 6.- Geo-climatic visualization of active power losses in transmission lines, 118-nodes

Fig. 7 shows the transmission line temperatures obtained with the WD-PF. It is observed that a factor that considerably influences the temperature in the transmission lines obtained by the WD-PF formulation, is the convective heat loss caused mainly by the presence of wind, causing lower line temperatures as observed in Wisconsin.

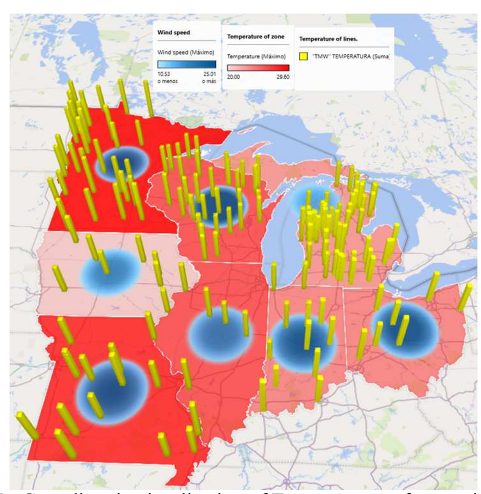

Fig. 7.- Geo-climatic visualization of Temperatures of transmission lines, 118-nodes

VII. Conclusions

Electrical active power losses are of paramount importance to the electrical industry due to the large number of monetary losses they represent. The knowledge of areas vulnerable to electrical losses or power congestion due to high conductor temperatures is usually closely related to climate changes and meteorological phenomena. In this project, some meteorological variables are considered within the study of power flows to obtain the active power electrical losses and line temperatures, presented in a complementary geographic visualization scheme, where the relationship between climate and electrical behavior can be identified in a simpler and more attractive way.

A power flow model is proposed that integrates a first approximation to the model a regulating transformer fed with meteorological data from the Internet. The open access to information reduces costs and can be implemented in real cases. The results presented show power losses considering multiple environmental variables and voltage regulation at different nodes. An innovative way to visualize system power losses has also been presented. The results suggest that ambient temperature and wind speed play a key role in influencing active power losses and temperature in transmission lines. Finally, it has been shown that reactive power losses are less sensitive to climatic changes.

IX.- References

[1] W. Williams, «Weather Normalization of Power System Reliability Indices,,» *IEEE Power Engineering Society General Meeting, Tampa, FL, USA,* 2007.

[2] U. news, 2019. [En línea]. Available: https://news.un.org/es/story/2019/07/1459821.

[3] California Independent System Operator, 2020

[4] S. Foss, S. Lin, A. Maraio and H. Schrayshuen, «Effect of variability in weather conditions on conductor temperature an dynamic rating of transmision lines,,» IEEE Transactions on power delivery, vol. 3, no 4, pp. 1832 - 1841, 1988.

[5] R. Stephen, «Thermal behaviour of overhead conductors,» Technical brochure, 2002.

[6] R. Santos, A. Exposito and F. P. Sanchez, «Assesment of conductor thermal models for grid studies,» IET Generation, transmission&distribution, vol. 1, no 1, pp. 155 - 161, 2007.

[7] S. Frank and M. Sexauer, «Temperature depend Power Flow,» IEEE Transactions on power systems, vol. 28, no 4, pp. 4007 - 4018, 2013.

[8] M. Bockarjova and G. Andersson, «Transmission line conductor temperature impact on state estimation accuracy,» de 2007 IEEE Lausanne Power Tech, Lausanne, Switzerland, 2007.

[9] P.Wang, H, Ma and Z. Han, « Dynamic Thermal Analysis of High-Voltage Power Cable Insulation for Cable Dynamic Thermal Rating» IEEE Access ., vol. 7, nº 4, pp. 2169-56106, 2019

[10] H. Yip, G.Lloyd and S. Jupe,« Dynamic thermal rating and active control for improved distribution network utilisation» 10th IET International Conference on Developments in Power System Protection (DPSP 2010). Managing the Change, Manchester, 2010.

[11] A. Ahmed,. J. Stevens and R. Rayudu, «Weather dependent power flow algorithm for accurate power system analysis under variable weather conditions,» IEEE Transactions on power systems ., vol. 34, nº 4, pp. 2719 - 2729, 2019

[12] J. Hong y K. W. Sup, «Weather impacts on electric power load: parcial phase synchronizacion analysis,» Meteorological applications, vol. 22, no 4, pp. 811-816, 2015.

[13] J. Cao, W. Du and F. Wang, «Weather-based optimal power flow with wind farms integration,» IEEE Transactions on Power Systems, vol. 31, no 4, pp. 3073 - 3081, 2016.

[14] A. Ahmed, F. MacFadden and R. Rayudu, «Transient stability study incorporating weather effects on conductors,» de IEEE Power & Energy Society General Meeting (PESGM), Portland, OR, 2018.

[15] C. Chen, J. Wang and D. Ton, «Modernizing Distribution System Restoration to Achieve Grid Resiliency Against Extreme Weather Events:An Integrated Solution», Proceedings of the IEEE, , vol. 105, no 7, pp. 1267, 2017.

[16] H. Kaur, S. Brar and J. Jaswinder, «Optimal power flow using power world simulator 2010 IEEE Electrical Power & Energy Conference, Halifax, NS, Canada, 2010.

[17] A. Raje, «Deregulation analytics for security assessment in IEEE 118-bus system using modular power flow,» 2016 International Conference on Electrical Power and Energy Systems (ICEPES), Bhopal, India, 2016

[18] A. Salam and M. Rashid, «Transient Stability Analysis of a Three-machine Nine Bus Power System Network ,» Engineering letters, Vol. 22 13, no 1, pp. 1-7, 2014.

[19] IEEE Standard, «IEEE Standard for calculating the current-temperature relationship of Bare Overhead Conductors-738,,» IEEE Power and Energy Society, 2012.

[20] A. Canepa, B. Delfino, M. Invernizzi and P. Pinceti, «Voltage regulation via automatic load tap changing transformers: Evaluation of voltage stability conditions,» Electric Power Systems Research, vol. 13, no 2, pp. 99-107, 1987.

[21] A. Olukayode, A. Warsame, P. Cofie and J. Fuller, «Analysis of the load flow problem in power system planning studies,» Energy and Power Engineering, vol. 7, no 10, pp. 509-523, 2015.

[22] H. Saadat, Power system analysis, New York, Unites State: McGraw- Hill, 1976.

[23] F. Melad. and J. M. Exposito, «meteored.mx,» 2010. [En línea]. Available: ttps://www.meteored.mx/gn/8775350.htm..

[24] Open Weather global services, «https://openweathermap.org/about-us»

[25] M. Iacob and C. Bejan, «SCADA automation system laboratory, elements and applications,» 2009 7th International Symposium on Intelligent Systems and Informatics, Subotica, Serbia, 2009.

[26] R. R. Cramen Au, Microsoft Mapping Geospatial development in windows 10 with Bing Maps and C#, 1484214439: Apress, 2015.

[27] Peña, C. Martinez-Anido and B. Hodge, «An Extended IEEE 118-Bus Test System With High Renewable Penetration», IEEE Transactions on Power Systems, vol. 33 no.1, pp. 281-289, 2017.